CORRELATION BETWEEN THE DISCHARGE REGIME AND HEAT GENERATION IN A SURFACE DBD PLASMA ACTUATOR

R. TIRUMALA[1]*, N. BENARD[1], E. MOREAU[1], M. FENOT[1], G. LALIZEL[1], E. DORIGNAC[1]

[1] Institut PPRIME, Université de Poitiers (CNRS UPR 3346, ISAE-ENSMA),
Boulevard Marie et Pierre Curie, BP30179, 86962 Futuroscope, France
*rakshit.tirumala.kumara@univ-poitiers.fr

ABSTRACT

Despite the extensive research on the application of dielectric barrier discharge based plasma actuators for active flow control, there is little work on their thermal characteristics as well as their use in heat transfer applications. This paper studies the effect of the shape of the AC discharge cycle on the thermal characteristics of a thick dielectric based DBD actuator. Simultaneous infrared (IR) thermography measurements and iCCD imaging is conducted for four different input waveforms to observe for changes in the temperature distribution on the dielectric surface. Global variations of temperature and local correlation between temperature and light intensity are analysed in relation to the previously documented differences in discharge characteristics for the four waveforms.

1. INTRODUCTION

Over the last decade, the use of DBD based plasma actuators as active flow control mechanisms has gained significant interest in the aerodynamic community [1,2]. Their effectiveness in controlling flow separation over airfoils is well established, at least in laboratory conditions. However, despite this success, there have been few efforts in adopting the technology for control and enhancement of heat removal through forced air convection. Corona discharge driven ionic winds have been well studied in small, millimeter scales as potential heat transfer mechanisms for electronics cooling [3]. There has been little effort in translating this, with DBDs, to the scale encountered in internal flow control for aeronautical applications. Previously, Joussot et al. [4] conducted infrared measurements of the temperature on the dielectric surface of a DBD actuator (0.6 mm in thickness) and characterised it against the input voltage and frequency measuring a temperature rise of 40-60°C. Dong et al. [5] and Stanfield et al. [6] conducted spectroscopic measurements of a DBD actuator to determine the rotational temperature of the gas above the grounded electrode and reported gas temperatures of 100 - 200°C.

A DBD has two main discharge regimes - the streamer regime corresponding to the positive going part of the AC cycle and a glow regime on the negative going part of the cycle. It has been observed that flow generation and induced thrust is stronger in the negative going cycle (or glow regime) [7]. The shape of the input waveform has also been shown to alter the discharge characteristics as well as the induced flow velocity [7,8]. In this study, simultaneous IR thermography measurements of the dielectric temperature and iCCD imaging of the discharge are conducted on a 3 mm thick dielectric based DBD actuator to analyse the effects of the discharge regime and shape of the input waveform on the temperature distribution over the dielectric surface. The overall change in the temperature is observed to be related to the regimes of the discharge cycle and the previously documented changes in the discharge characteristics as a result of the variations in input AC waveform [7,8].

2. EXPERIMENTAL SETUP

The plate-to-plate DBD actuator consists of two thin metallic electrodes mounted on either side of a dielectric barrier, with a high AC voltage applied to the top electrode and the bottom electrode being grounded. In the present study, the dielectric barrier is made of 3-mm thick PMMA. The width of the top, high voltage electrode (also called active electrode) is 20 mm and that of the grounded electrode is 50 mm. The gap between the edges of the two electrodes is 2 mm. Both the electrodes are 80 µm thick and have a span wise length of 80 mm. The grounded electrode is encapsulated in epoxy resin to ensure that the discharge occurs only on the top surface. To obtain accurate emissivity for IR thermography, the surface of the dielectric is coated with a layer of non-conductive black paint with a known thermal emissivity (ε) of 0.95. The entire plate is covered on the back with a 25 mm thick layer of foam to provide a thermal insulation. For all the measurements, the actuator is positioned vertically, with the ionic wind flowing vertically upwards. Because ionic wind velocities of 5 m/s are generated, the influence of forced convection from the flow is assumed to dominate over natural convection. The experimental setup is shown in Fig. 1.

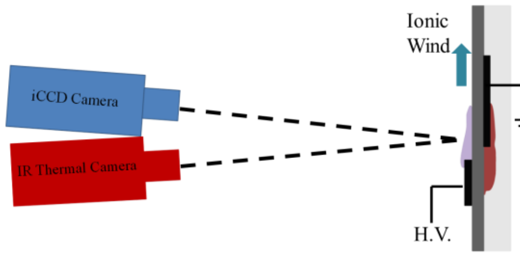

Fig. 1 Schematic of the experimental arrangement

The active electrode is supplied by a power amplifier (Trek, +/-30kV, 40mA) which is driven by a Hameg HM8310 function generator. The amplitude of applied voltage in all cases is 18 kV and frequency of the AC cycle is 1 kHz. The thermal images are obtained using an FLIR infrared camera system (spectral range 3.0 – 5.0 µm) after discharge operation for 240 seconds to achieve temperature steady state. The images are recorded at a rate of 1 frame/s. The discharge images are captured using a Pi-Max1 intensified CCD camera with a Nikkor 100 mm lens synchronized to the function generator. A 150 µs time window of the AC cycle corresponding to the glow region of the discharge is imaged and a cumulative of 10 cycles is acquired to improve light captured. It was observed that the locations of the glow spots were invariant during the discharge run, which made the accumulation admissible.

3. RESULTS AND DISCUSSION

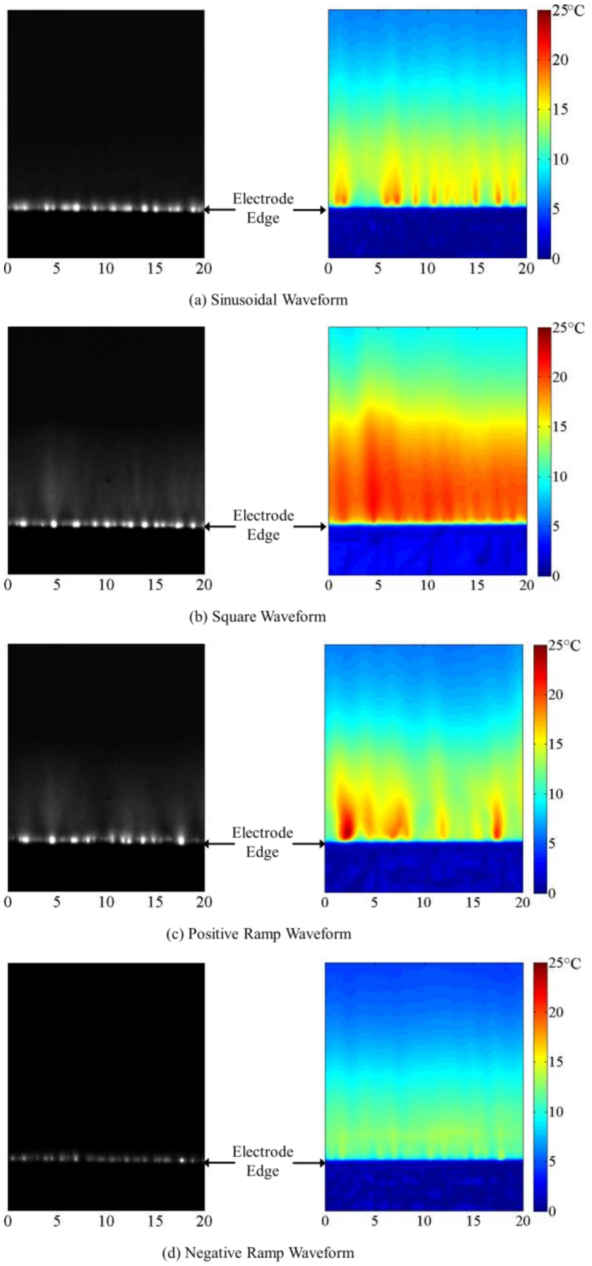

Fig. 2 Figure showing the discharge image (left) and temperature (ΔT) distribution (right) for (a) sinusoidal, (b) square, (c) positive ramp and (d) negative ramp waveforms. The temperatures are at t = 240 s.

Fig. 2 shows the discharge image and temperature distribution near the electrode edge for a span of 20 mm for four different waveforms. To account for changing initial (or ambient) conditions (T_0), instead of the absolute temperature (T), the change in temperature ($\Delta T = T-T_0$) is reported with a uniform range of 0-25 °C maintained for all waveforms. From the measured data, it was observed that the maximum temperature rise (ΔT_{max}) occurred near the electrode edge and is higher in the case of the square and positive ramp waveforms (22 ºC and 24 ºC respectively) compared to the sine and negative ramp waveforms (20 ºC and 15 ºC respectively). This is not in relation with the power consumption for the four waveforms. Jolibois and Moreau [8] showed that for a particular voltage, the square waveform consumed the highest power, followed by sine, negative and positive ramp waveforms. The maximum value of local temperature is instead observed to be related to the intensity of the glow discharge. As studied by Benard and Moreau [7], the glow discharge is enhanced when the applied high voltage has a waveform in which the negative slope has a stronger gradient (square and positive ramp). Figure 2 suggests that this also increases the heat transfer and produces the higher values of ΔT, demonstrating that the heating is more dominant during the glow discharge regime of the AC cycle.

The glow regime of the discharge cycle is also observed to have influence on the temperature distribution on a local scale near the electrode edge. For the four input waveforms, Fig. 3 plots the temperature and light intensity along the electrode edge normalized to their respective minima and maxima. A correlation is observed between the two, with the peaks and troughs in temperature corresponding to the ones in light intensity. Since the discharge image is instantaneous and the temperature is a cumulative effect of 240 s, the final temperature profile is seen to be an envelope covering the peaks in the light intensity. A similar comparison was made with light intensity from the streamer regime of the discharge but no such alignment was observed between the peaks.

It can also be observed from the Fig. 2 that for the square waveform, the temperature is more uniform and has a smaller streamwise gradient than the other waveforms. Fig. 4 plots the streamwise variation of the temperature distribution normalized to their respective maxima. The temperature is measured at a y-location corresponding to a glow spot or temperature hotspot. The plot shows that the square waveform retains the high temperature for a longer distance, with the positive ramp having the quickest drop. The previous work by Benard and Moreau [7] also demonstrated the difference in the streamwise component (u) of ionic wind velocity for the four waveforms. The square waveform was observed to have the highest mean velocity, followed in order by sine, negative and positive ramp waveforms.

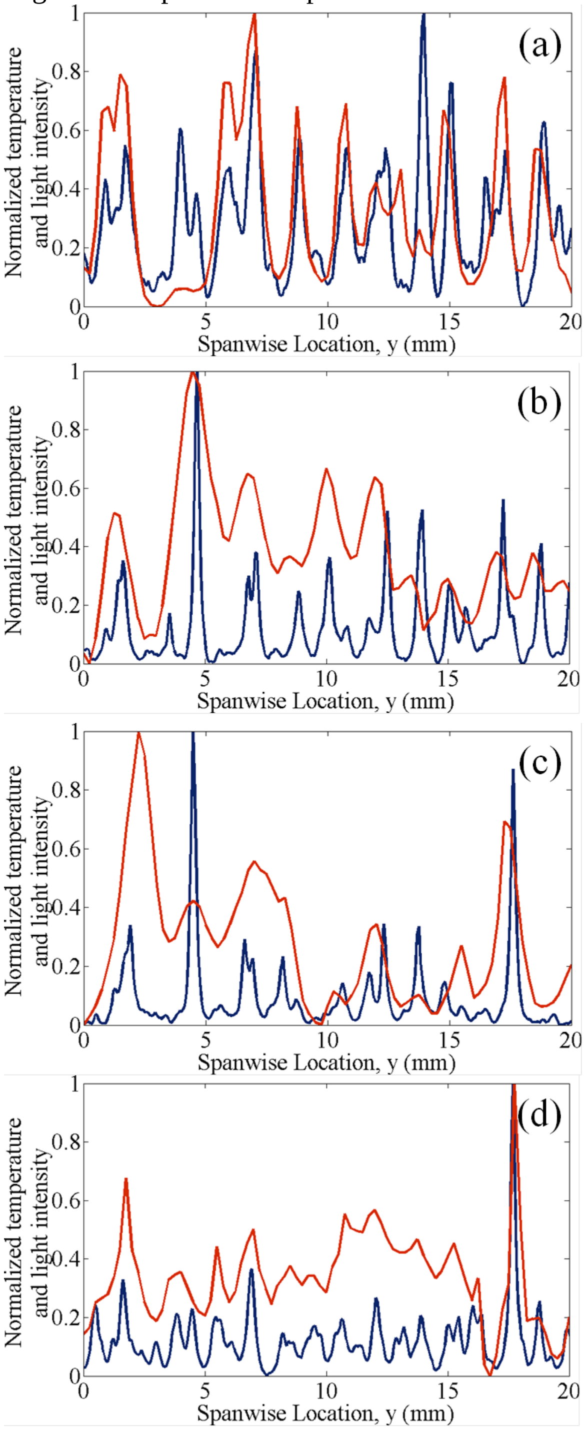

Fig. 3 Plots of normalized temperature (red —) and light intensity (blue —) for a 20 mm span along the edge of the active electrode for (a) sine, (b) square, (c) positive ramp and (d) negative ramp waveforms. The temperatures are at t = 240 s.

Jolibois and Moreau [8] demonstrated that the plasma extension, defined as the downstream location (x) where the maximum ionic wind velocity is measured, is highest for the square waveform, with the sine, negative and positive ramp waveforms following. As evidenced from Fig. 4, this seems to have a direct impact on the temperature gradient over the dielectric surface. The plot shows that near the electrode edge (x = 0), the square waveform retains the high temperature for a longer distance, with the positive ramp having the quickest drop. The ionic wind velocity is also related to the gradients in temperature through the convection coefficient. This effect is suggested by Fig. 4.

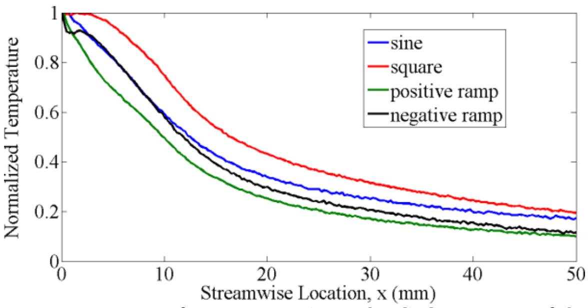

Fig. 4 Variation of temperature (normalized) downstream of the electrode for the four input waveforms. The temperatures are at t = 240 s.

4. CONCLUSIONS

This work studied the effects of the input high voltage AC waveform on the temperature characteristics of a dielectric barrier discharge actuator. The shape of the waveform was observed to influence the rise in temperature (ΔT) and also its distribution over the dielectric surface. Corresponding to the changes observed in the discharge [7], the temperature increase was also found to be higher in cases where the glow regime was stronger (square and positive ramp waveforms). On a smaller scale, correlation was also observed between the glow discharge part of the cycle and the temperature variation near the active electrode. It can be inferred that the temperature distribution is predominantly influenced by the glow regime of the discharge cycle, which is also known to have a stronger influence on the induced ionic wind. It cannot be argued beyond doubt that only the glow regime of the DBD cycle generates heat and the streamer regime of the discharge plays no role in heat generation. But given the above evidence of correlation near the electrode's edge and the relationship of the temperature rise with glow intensity, it can be speculated that the glow regime contributes the majority of direct heat injection in this region. The streamers are thin filamentary channels of ions and exist only for a very short duration (~30 ns) [1]. Thus it is possible that no direct heat transfer occurs from the streamers to the dielectric surface. The glow spots are corona like and occur at locations of intensified electric fields. It is possible that the localised ionization at these spots contributes direct heat injection into the dielectric surface.

ACKNOWLEDGEMENTS

Work was funded by the French government program “Investissements d'avenir” (LABEX INTERACTIFS, reference ANR-11-LABX-0017-01).

REFERENCES

[1] N. Benard and E. Moreau, "EHD force and electric wind produced by surface dielectric barrier discharge plasma actuators used for airflow control," in 6th AIAA Flor Control Conference, New Orleans, 2012.
[2] T. C. Corke, C. L. Enloe and S. P. Wilkinson, "Dielectric Barrier Discharge Plasma Actuators for Flow Control," Annual Review of Fluid Mechanics, **42**, pp. 505-529, 2010.
[3] D. B. Go, R. A. Maturana, T. S. Fisher and S.V. Garimella, "Enhancement of external forced convection by ionic wind," International Journal of Heat and Mass Transfer, **51**, pp. 6047-6053, 2008.
[4] R. Joussot, D. Hong, H. Rabat, V. Boucinha, R. Weber-Rozenbqum and A. Leroy-Chesneau, "Thermal Characterization of a DBD Plasma Actuator: Dielectric Temperature Measurements Using Infrared Thermography," in 40th Fluid Dynamics Conference and Exhibit, Chicago, 2010.
[5] B. Dong, J. M. Bauchire, J. M. Pouvesle, P. Magnier and D. Hong, "Experimental study of a DBD surface discharge for the active control of subsonic airflow," *Journal of Physics D: Applied Physics*, **41**, p.155201, 2008.
[6] S. A. Stanfield, J. Menart, C. DeJoseph, R. L. Kimmel and J. R. Hayes, "Rotational and Vibrational Temperature Distributions for a Dielectric Barrier Discharge in Air," AIAA Journal, **47**, no. 5, pp. 1107-1115, 2009.
[7] N. Benard and E. Moreau, "Role of electric waveform supplying a dielectric barrier discharge plasma actuator," Applied Physics Letters, **100**, p. 193503, 2012.
[8] J. Jolibois and E. Moreau, "Enhancement of the electromechanical performances of a single dielectric barrier discharge actuator," IEEE Trans. Dielectrics and Electrical Insulation, **16**, no. 3, pp. 758-767, 2009.